Japanese Journal of Applied Physics
Vol. 43, No. 5B, 2004, pp. 3220–3226

Cross-Sectional Elasticity Imaging of Carotid Arterial Wall in Short-Axis Plane by Transcutaneous Ultrasound

Nozomi NAKAGAWA, Hideyuki HASEGAWA* and Hiroshi KANAI

Graduate School of Engineering, Tohoku University, Sendai 980-8579, Japan

(Received November 20, 2003; accepted January 30, 2004; published May 28, 2004)

We have developed the *phased tracking method* [H. Kanai, M. Sato, Y. Koiwa and N. Chubachi: IEEE Trans. UFFC **43** (1996) 791.] for measuring the minute change in thickness during one heartbeat and the elasticity of the arterial wall with transcutaneous ultrasound. When this method is applied to a plane perpendicular to the axis of the artery (short-axis plane) using a linear-type probe, only an ultrasonic beam which passes through the center of the artery coincides with the direction of the change in thickness. At other beam positions, the wall motion cannot be accurately tracked because the direction of wall expansion slips off the beam. To obtain the cross-sectional image of elasticity in the short-axis plane using transcutaneous ultrasound, in this paper, the directions of ultrasonic beams are designed so that each beam always passes through the center of the artery; thus, they always coincide with the direction of the wall expansion. In basic experiments, the accuracy in elasticity measurement was evaluated using a silicone rubber tube. In *in vivo* experiments, the minute change in wall thickness was measured along each ultrasonic beam, and the cross-sectional image of elasticity was obtained in the short-axis plane with transcutaneous ultrasound. [DOI: 10.1143/JJAP.43.3220]

KEYWORDS: elasticity of arterial wall, short-axis plane, small change in wall thickness

1. Introduction

Recently, the increase in the number of patients suffering from myocardial infraction or cerebral infraction has become a serious social problem. Therefore, it is important to diagnose atherosclerosis in an early stage because such circulatory diseases are mainly caused by atherosclerosis. Because the elasticity of the arterial wall changes as atherosclerosis develops,[1] the evaluation of the regional elasticity of the arterial wall using ultrasound is useful for the diagnosis of atherosclerosis.

Ultrasound B-mode imaging is widely used for the repetitive diagnosis of atherosclerosis because it is non-invasive and patients have few difficulties. Using the ultrasound B-mode image, the shape and the size of atherosclerotic plaque on the arterial wall can be observed in real time, but it is difficult to evaluate the stability of the plaque quantitatively. To evaluate the vulnerability of atherosclerotic plaque, we have developed a method, the *phased tracking method*, for measuring the minute change in wall thickness during one heartbeat and the regional elasticity of the arterial wall with transcutaneous ultrasound.[2–5]

In this method, when the ultrasonic beam is not coincident with the direction of the change in thickness, the wall motion cannot be accurately tracked because the direction of wall expansion slips off the beam. Therefore, this method is efficient if applied to a plane parallel to the axis of the artery (the long-axis plane as shown in Fig. 1) using a linear-type probe because the region where the ultrasonic beam is perpendicular to the arterial wall is wider than that perpendicular to the axial direction of the artery (the short-axis plane as shown in Fig. 1). However, it is difficult to diagnose the entire portion of the plaque with only the measurement in the long-axis plane. Therefore, it is necessary to measure the elasticity of the plaque in the short-axis plane in addition to the measurement in the long-axis plane.

*E-mail address: hasegawa@us.ecei.tohoku.ac.jp

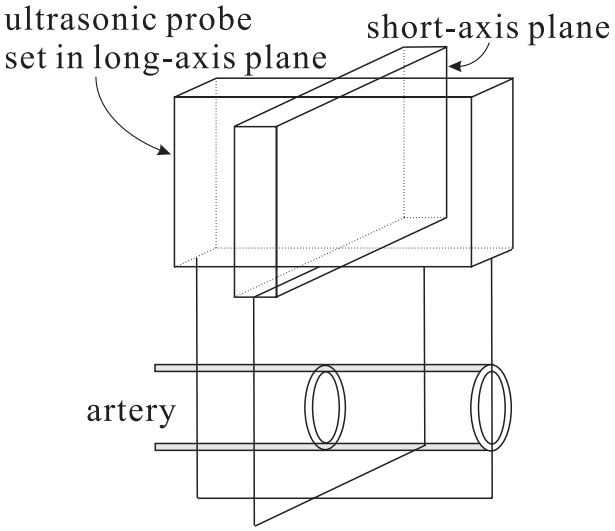

Fig. 1. Schematic of probe positioning.

A method for measuring the cross-sectional image of the elasticity of the arterial wall in the short-axis plane using intravascular ultrasonography (IVUS) has been reported. De Korte and coworkers measured the strain of the arterial wall caused by the change in inner pressure and calculated the elasticity during cardiac diastole when the motion of the IVUS probe caused by the pulsatile flow is negligible.[6,7] However, the elasticity can be estimated only during cardiac diastole with this method. Mita and coworkers developed a method for measuring the strain during an entire heart cycle by compensating the change in the position of the IVUS probe caused by pulsatile flow.[8] Although these methods are useful for evaluating the vulnerability of the plaque, they are not suitable for repetitive diagnosis due to invasion during catheterization.

When the artery is measured transcutaneously in the short-axis plane by conventional linear scanning, only an ultrasonic beam which passes through the center of the artery coincides with the direction of wall motion (change in

wall thickness). At other beam positions, wall motion cannot be accurately tracked because the direction of wall expansion slips off the beam. Watanabe and coworkers showed that the change in the thickness of the arterial wall can be measured accurately in the region of ±0.45 mm around the ultrasonic beam which passes through the center of the artery by setting the focal depth deeper than the outer surface of the posterior wall.[9] However, to measure the change in wall thickness accurately within a wider region in the short-axis plane, each ultrasonic beam should be scanned so as to be perpendicular to the wall.

In this paper, for the assessment of the cross-sectional elasticity image in the short-axis plane, the directions of the ultrasonic beams are designed so that each beam always passes through the center of the artery and the direction of each beam becomes always perpendicular to the arterial wall.

2. Principles

2.1 Beam steering

Figure 2 shows the schematic of beam scanning. In this study, the ultrasonic beams are transmitted in the $(N+1)$ directions and designed so that each beam passes through the center, O, of the artery. Under such a setting, the ultrasonic beams are always perpendicular to the arterial wall if the cross-section of the artery lumen can be assumed to be a circle. The beam scanning system is designed as follows: The distance, d_k, from the center, c_k, of the transmit aperture of the k-th beam ($k = -N/2, \cdots, 0, \cdots, N/2$) to the center of the probe is expressed as

$$d_k = 0.4 \cdot k \quad [\text{mm}]. \tag{2.1}$$

The beam angle, θ_k, of the k-th beam is expressed as

$$\theta_k = \arctan\frac{d_k}{L_i} \quad [\text{rad}], \tag{2.2}$$

where L_i is the distance from the surface of the probe to the point O. In this paper, L_i is variable from 8.5 mm to 21.5 mm with a pitch of 1 mm ($i = 1, 2, \cdots, 14$). The focal distance, f_k, of the k-th beam is defined by

$$f_k = \frac{L_i}{\cos\theta_k} + 9 \quad [\text{mm}]. \tag{2.3}$$

In eq. (2.3), 9 mm is added to the distance from c_k to O so that the focal depth becomes deeper than the posterior wall. The beam width at the posterior wall is increased by this setting, and a wider beam is more robust against wall motion which slips off the beam.[10] By changing the distance, L_i, each ultrasonic beam can be perpendicular to the arterial wall even in the case of a subject with a different distance from the skin surface to the artery.

2.2 Calculation of change in wall thickness

Using the *phased tracking method*,[2] the velocities of inner and outer surfaces were obtained from the phase shift, $\Delta\hat{\theta}(t)$, between ultrasonic pulses transmitted and received with a repetition interval T as

$$\hat{v}(t) = -\frac{c_0}{2\omega_0}\frac{\Delta\hat{\theta}(t)}{T}, \tag{2.4}$$

where ω_0 and c_0 are the center angular frequency of the ultrasonic pulse and the speed of sound, respectively.

From the displacements, $x_A(t)$ and $x_B(t)$, of two points, which are set in the arterial wall along an ultrasonic beam, the change in thickness, $\Delta h(t)$, between these two points is obtained as

$$\Delta\hat{h}(t) = \hat{x}_A(t) - \hat{x}_B(t) \tag{2.5}$$

$$= \int_0^t \{\hat{v}_A(t) - \hat{v}_B(t)\}\mathrm{d}t. \tag{2.6}$$

3. Basic Experiments

Figure 3 shows the schematic of the basic experimental system. The change in the wall thickness of a silicone rubber tube (static elastic modulus: 5.7 MPa, sound speed: 992 m/s, inner diameter: 10 mm, outer diameter: 13 mm) caused by

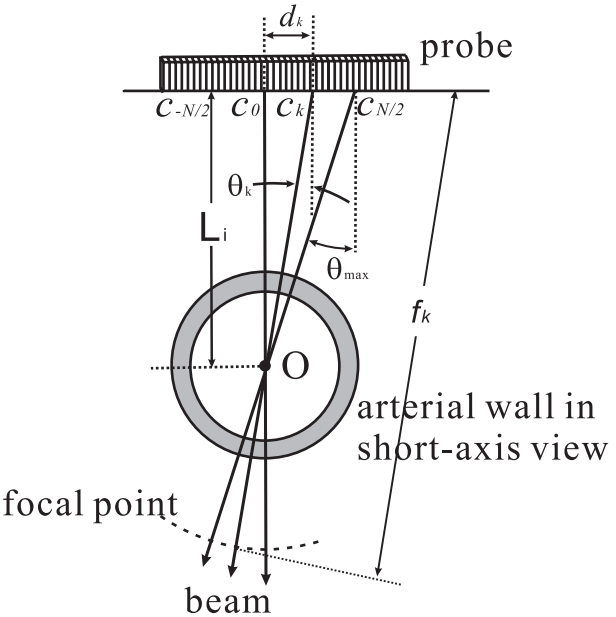

Fig. 2. Schematic of beam scanning.

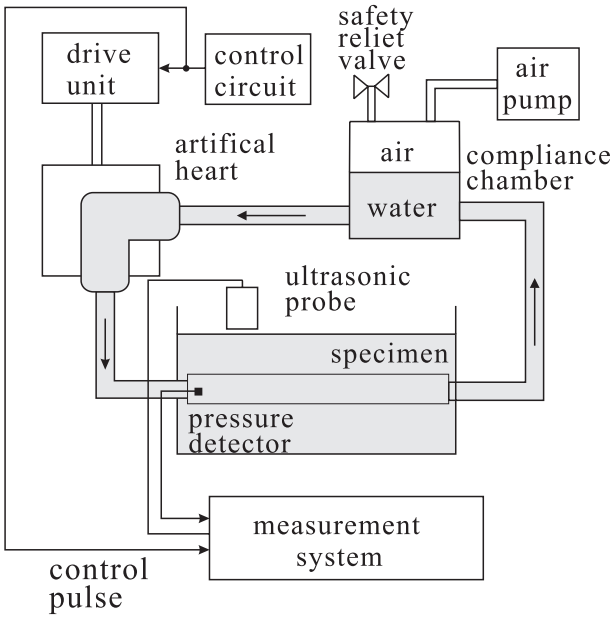

Fig. 3. Schematic of basic experimental setup.

pulsatile flow generated by an artificial heart is measured in the short-axis plane with a linear-type probe (center frequency: 10 MHz). Figures 4(a) and 4(b) show the B-mode images measured by a conventional linear scanning method and the proposed method ($L_i = 11.5$ mm, the largest beam angle $\theta_{max} = 24.3°$), respectively. In Fig. 4, beams at positions l_1 and l_2 measured the same regions of the posterior wall, as measured by beams at positions l'_1 and l'_2.

M-mode images, signals driving the artificial heart, inner pressures, velocities of inner and outer surfaces and changes in wall thickness measured at beam positions l_1, l_2, l'_1 and l'_2 in Fig. 4 are shown in Figs. 5(a), 5(b), 6(a) and 6(b), respectively.

By linear scanning, as shown in Fig. 5(a-6), the change in thickness measured at the beam position l_1 is measured with high reproducibility, and its waveform correlates well with that of the change in inner pressure. At the beam position l_2, where the ultrasonic beam was not perpendicular to the arterial wall, the amplitude of the change in thickness, shown in Fig. 5(b-6), was different from that measured at l_1 because the direction of wall expansion due to the pulsatile flow slipped off the beam.

On the other hand, using the proposed method, the changes in the thickness of the silicone rubber tube, at both beam positions l'_1 and l'_2 were measured with the similar amplitude, waveform and high reproducibility as shown in Figs. 6(a-6) and (b-6). At the position l'_2, a beam cannot be scanned so as to be perpendicular to the wall by linear scanning.

Figure 7(a-1) shows the mean value and the standard deviation of the maximum change in thickness for 5 heart beats measured in the region of ±2.2 mm (the number of beams: 27) around the beam which passes through the center of the silicone rubber tube.

Figure 7(a-2) shows the mean value and the standard deviation of the elasticity, which is obtained from the maximum change in thickness and the maximum change in inner pressure measured by the pressure sensor (NEC 9E02-P16). The beam number of 26 corresponds to the beam position l_2 shown in Fig. 4(a).

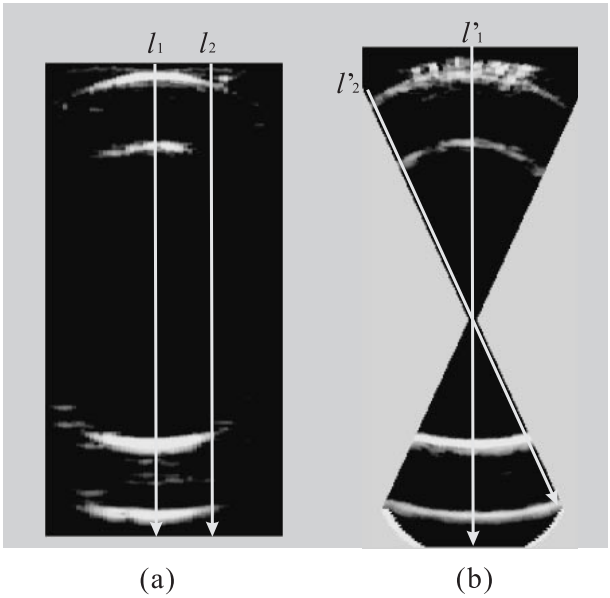

Fig. 4. B-mode images of a silicone rubber tube obtained by the conventional linear scanning method (a) and the proposed method (b).

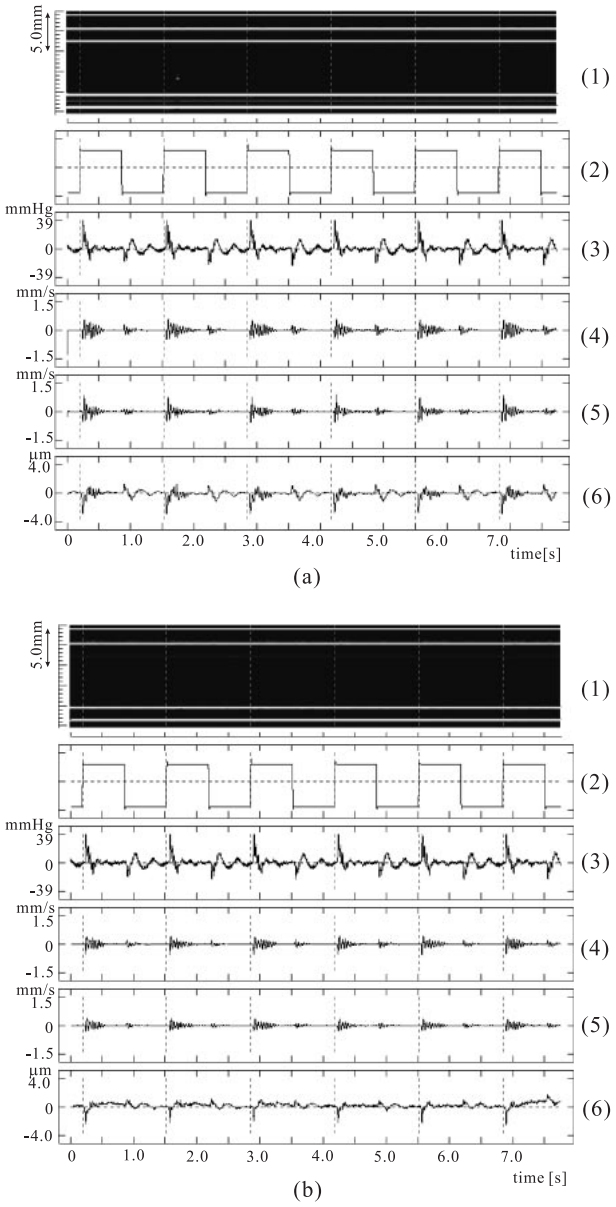

Fig. 5. Basic experimental results obtained by the conventional linear scanning method: (a) beam position l_1 in Fig. 4(a) and (b) beam position l_2 in Fig. 4(a). (1) M-mode image. (2) Signal driving the artificial heart. (3) Inner pressure. (4) Small vibration velocity of inner surface. (5) Small vibration velocity of outer surface. (6) Change in thickness.

Using linear scanning, the change in thickness was measured with sufficient reproducibility in the region which corresponds to 8 beams around the beam which passes through the center of the tube. As shown in Fig. 7(a-2), with respect to these 8 beams, mean values of the elastic modulus agreed well with those of the elastic modulus measured by a different static experiment (5.8 MPa), and the standard deviations were found to be small ((the standard deviation)/(mean value) ranged from 5.1 to 5.8% at these 8 beam positions).

In other beam positions, mean values of elastic modulus did not agree well with that obtained by the static experiment, and the standard deviations increased due to a decrease in the signal-to-noise ratio of the reflected ultra-

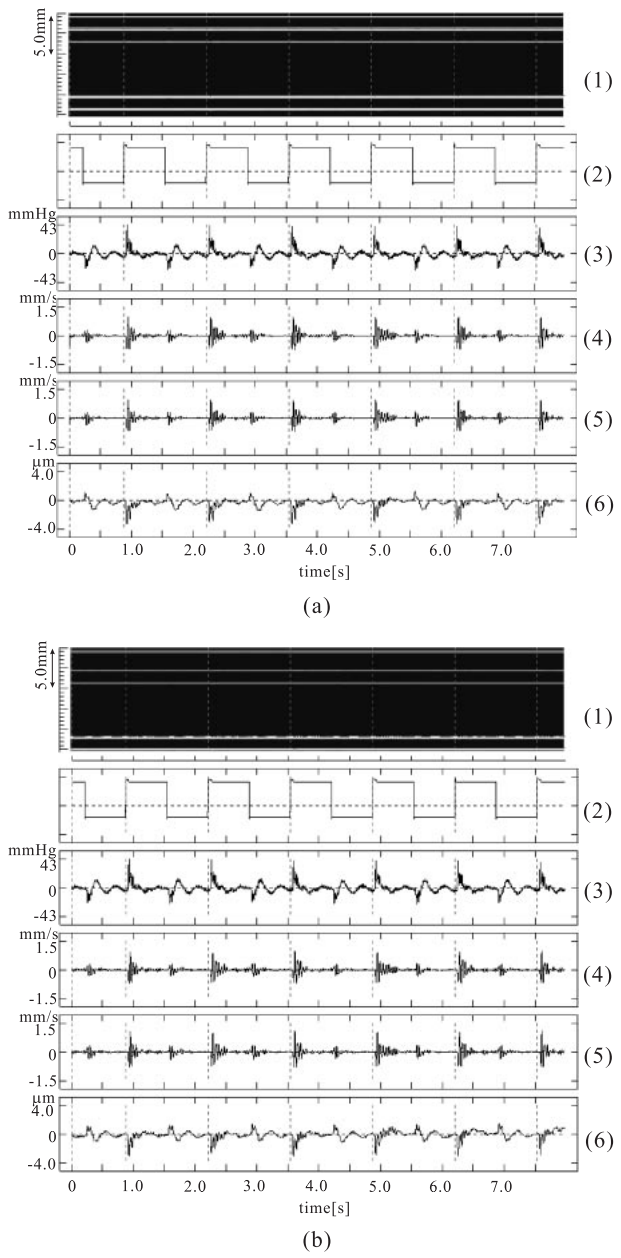

Fig. 6. Basic experimental results obtained by the proposed method: (a) beam position l'_1 in Fig. 4(b) and (b) beam position l'_2 in Fig. 4(b). (1) M-mode image. (2) Signal driving the artificial heart. (3) Inner pressure. (4) Small vibration velocity of inner surface. (5) Small vibration velocity of outer surface. (6) Change in thickness.

sonic waves. The ratio, $A(l_2)/A(l_1)$, of amplitudes, $A(l_1)$ and $A(l_2)$, of echoes at the beam positions l_1 and l_2 in Fig. 4, was 0.33.

Figure 7(b-1) shows the mean value and the standard deviation of the change in thickness for 5 beats measured within the entire region of the B-mode image shown in Fig. 7(b-3) (number of beams: 53) using the proposed method, and the beam number of 27 corresponds to the beam position l'_2 shown in Fig. 4(b).

In Fig. 7(b-1), changes in thickness were measured with sufficient reproducibility at all beam positions ((the standard deviation)/(mean value) ranged from 0.28 to 5.3% at all beam positions). As well as the case of linear scanning, the mean value and the standard deviation of the elastic modulus were calculated as shown in Figure 7(b-2).

In Fig. 7(b-2), the mean value of the elastic modulus measured at each beam was close to 5.8 MPa which was measured by a different static experiment ((the standard deviation)/(mean value) ranged from 0.7 to 7.2%, and $A(l'_2)/A(l'_1)$ is 0.97). The mean values of elastic moduli measured at all beams for 5 beats was 5.6 MPa.

These results indicate that the elastic modulus of the tube can be accurately measured in the short-axis plane by the proposed method.

4. *In vivo* Experiments

The change in the thickness of a human common carotid artery of a 29-year-old male was measured in the short-axis plane. The B-mode image measured by the 10 MHz linear-type probe is shown in Fig. 8. The B-mode images were drawn at the time of the R-wave of the electrocardiogram. Figures 8(a) and 8(b) show B-mode images measured by the conventional linear scanning method and the proposed method, respectively. In this experiment, $L_i = 15.5$ mm and the largest beam angle, $\theta_{\max}$, was 21.2°. In Fig. 8, beams at positions l_1 and l_2 measured the same regions of posterior wall, as measured by beams of the positions l'_1 and l'_2.

As shown in Fig. 8(a), using the conventional linear scanning method, an echo reflected from the lumen-intima interface was recognized only in the region of about 0.9 mm around the ultrasonic beam, l_1, which passes through the center of the artery. At other beam positions such as l_2, surrounded by a circle in Fig. 8(a), an echo from the lumen-intima interfaces was barely recognized because the ultrasonic beam was not perpendicular to the wall. On the other hand, as shown in Fig. 8(b), echoes from the lumen-intima interface were clearly recognized at all ultrasonic beam positions by controlling each beam so as to be perpendicular to the wall. As a result, echo from the lumen-intima interface could be recognized in a wider region of 2.0 mm.

M-mode images, electrocardiograms, velocities at the intimal side and the adventitial side of the posterior wall, and changes in wall thickness measured at beam positions l_1, l_2, l'_1 and l'_2 in Figs. 8(a) and 8(b) are shown in Figs. 9(a), 9(b), 10(a) and 10(b), respectively. By linear scanning, as shown in Fig. 9(a-5), the change in thickness was measured with high reproducibility at the beam position l_1, where the ultrasonic beam was perpendicular to the arterial wall. However, at the beam position l_2, where the ultrasonic beam was not perpendicular to the arterial wall, the amplitude of the change in thickness was different from that measured at l_1 because the direction of wall expansion due to the heartbeat slipped off the beam. Moreover, the reproducibility during heartbeats was made worse by the decrease in the signal-to-noise ratio of the reflected ultrasonic waves. The ratio, $A(l_2)/A(l_1)$, of amplitudes $A(l_1)$ and $A(l_2)$ of echoes at the beam positions l_1 and l_2 in Fig. 8 was 0.059.

As shown in Figs. 10(a-5) and (b-5), using the proposed method, the changes in the thickness of the arterial wall caused by the heartbeat were measured with a similar amplitude, waveform, and high reproducibility at both beam positions l'_1 and l'_2. (The ratio $A(l'_2)/A(l'_1)$ was 0.92.) At the beam position l'_2, a beam cannot be scanned so as to be perpendicular to the wall by linear scanning.

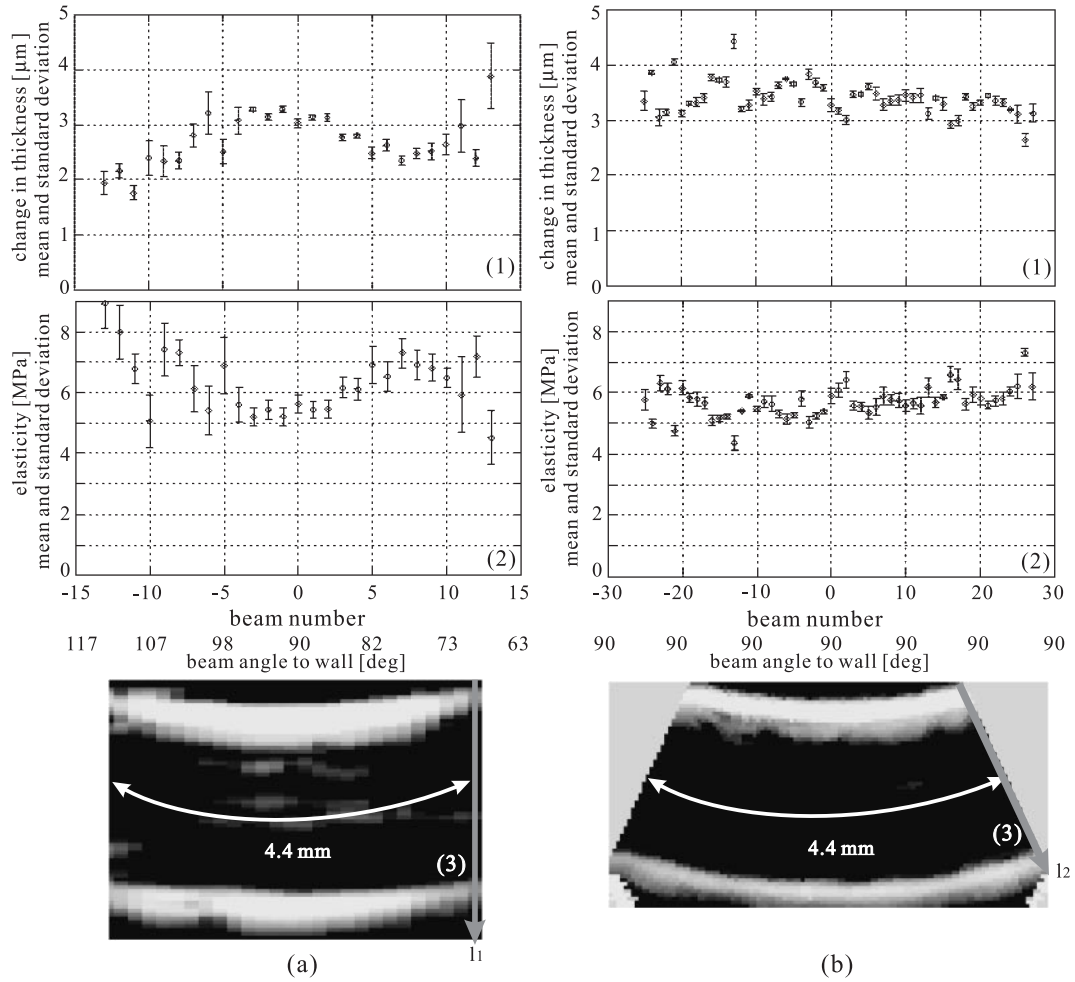

Fig. 7. Basic experimental results obtained by (a) the conventional linear scanning method and (b) the proposed method. (1) Mean value and standard deviation of the maximum change in wall thickness. (2) Mean value and standard deviation of the elastic modulus. (3) B-mode image of the corresponding region.

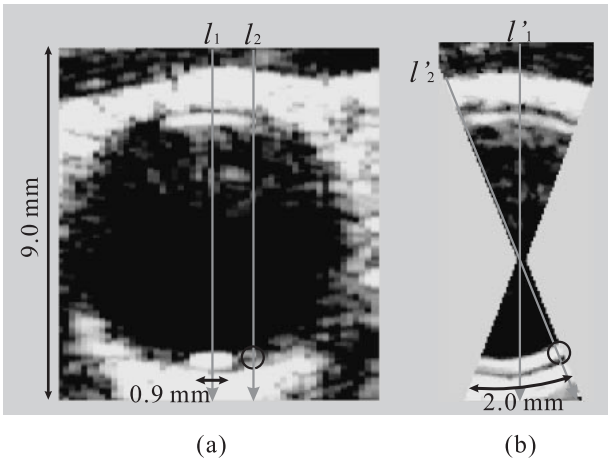

Fig. 8. B-mode images measured by the conventional linear scanning method (a) and the proposed method (b).

Figure 11(a-1) shows the mean value and the standard deviation of the change in thickness measured by the conventional linear scanning for 6 heartbeats in the region of ±1.0 mm (shown in Fig. 11(a-2), number of beams: 15) around a beam which passes through the center of the artery. Figure 11(b-1) shows the mean value and the standard deviation of the change in thickness measured by the proposed method for 6 heartbeats at all beam positions (number of beams: 30). Figures 11(a-2) and 11(b-2) show the B-mode images around the regions where changes in thickness were estimated by the conventional linear scanning method and the proposed method, respectively. As shown in Figs. 11(a) and 11(b), the beam numbers 7 and 15 correspond to the beam positions l'_1 and l'_2 shown in Fig. 8, respectively. In Fig. 11(a-1), the standard deviation of the change in thickness measured by the linear scanning was small in the region which corresponds to only 6 beams around the beam which passes through the center of the artery ((the standard deviation)/(mean value) ranged from 2.6 to 6.4% at the 6 beam positions). At other beam positions, the standard deviations were large, i.e., reproducibility worse.

Figure 11(b-1) shows the mean value and the standard deviation of the change in thickness measured by the proposed method for 6 heartbeats. Changes in wall thickness were measured with high reproducibility at all beam positions (width: 2.0 mm) ((the standard deviation)/(mean value) ranged from 1.5 to 12.1% at all beam positions). In Fig. 11(b-1), there are differences in mean values between beam positions. It is supposed that changes in wall thickness are actually inhomogeneous in the circumferential direction

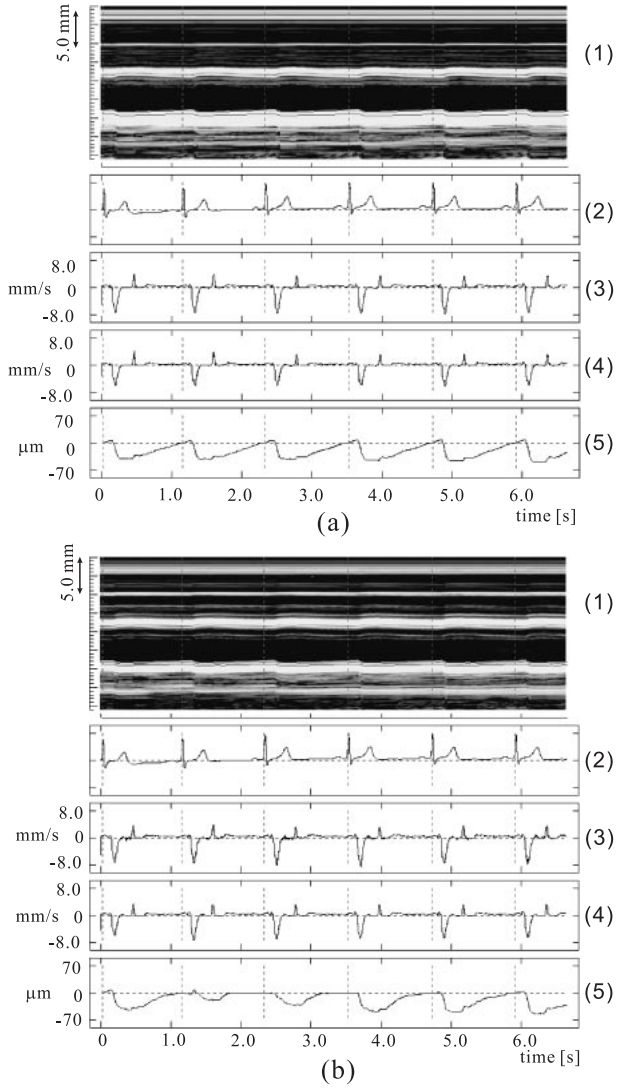

Fig. 9. *In vivo* experimental results obtained by the conventional linear scanning method: (a) beam position l_1 in Fig. 8(a) and (b) beam position l_2 in Fig. 8(a). (1) M-mode image. (2) Electrocardiogram. (3) Small vibration velocity on intima. (4) Small vibration velocity on adventitia. (5) Change in the thickness of the posterior wall.

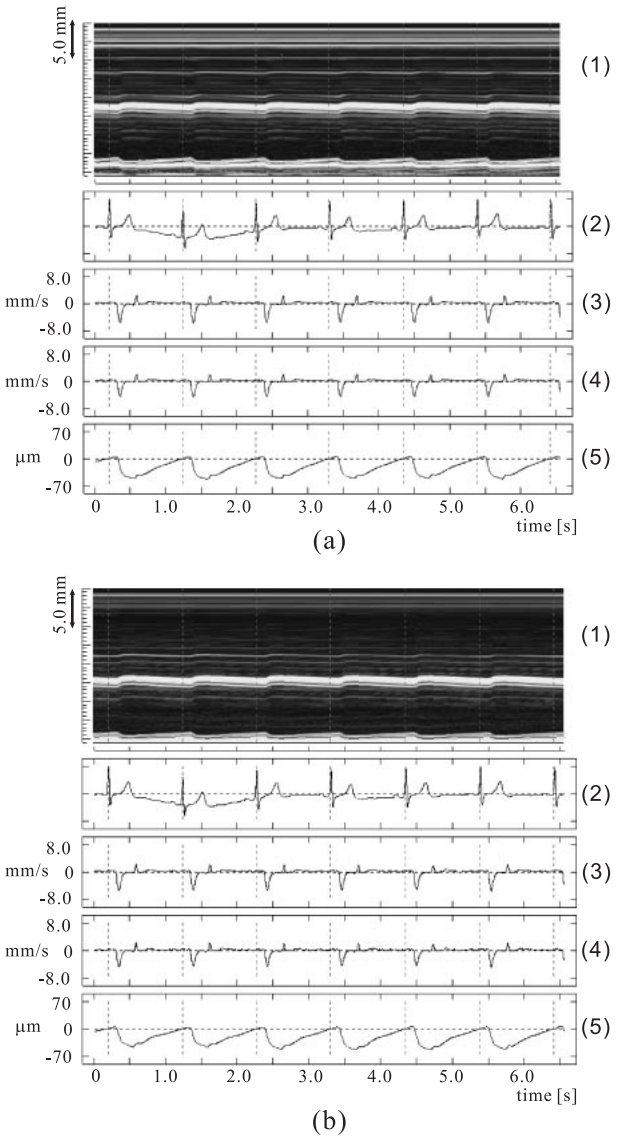

Fig. 10. *In vivo* experimental results obtained by the proposed method: (a) beam position l_1' in Fig. 8(b) and (b) beam position l_2' in Fig. 8(b). (1) M-mode image. (2) Electrocardiogram. (3) Small vibration velocity on intima. (4) Small vibration velocity on adventitia. (5) Change in the thickness of the posterior wall.

because of the facts that the accuracy of the proposed method was validated by basic experiments and the measured changes in thickness in Fig. 11(b-1) have high reproducibility for 6 heartbeats at all beam positions.

Figures 12(a) and 12(b) show the B-mode images of the carotid artery obtained by conventional linear scanning at two different angles. The regions shown by the yellow dotted lines and red dotted lines in Fig. 12(a) correspond to those shown in Fig. 12(b). Figures 12(c) and 12(d) show the cross-sectional images of elastic modulus measured in two different regions shown by yellow dotted lines and red dotted lines in Figs. 12(a) and 12(b), respectively. Figures 12(c) and 12(d) were measured at the same angles as Fig. 12(a) and 12(b), respectively. The elastic modulus is obtained by the maximum change in thickness and the pulse pressure measured at the upper arm. The resolution of the cross-sectional image of elastic modulus was 80 μm in the depth direction and $1.43^\circ \pm 0.5^\circ$ in the circumferential direction.

The region of the carotid artery between two red dotted lines in Fig. 12(b) was measured. Then, the probe was rotated about 20 deg along the neck, and the region between two yellow dotted lines in Fig. 12(a) was measured. It is recognized that the elasticity images of the regions between two green dotted lines shown in Figs. 12(c) and 12(d), which are measured by both measurements, correspond to each other. The mean value and the standard deviation of the measured elastic modulus shown in Figs. 12(c) and 12(d) were 0.18 ± 0.14 MPa and 0.2 ± 0.15 MPa, respectively.

From these results, using the proposed method, the elasticity distribution of the arterial wall can be measured transcutaneously within the wide region in the short-axis plane.

5. Conclusion

In this study, the ultrasonic beams are designed so that each beam is always perpendicular to the arterial wall in the short-axis plane. In basic experiments using a silicone rubber

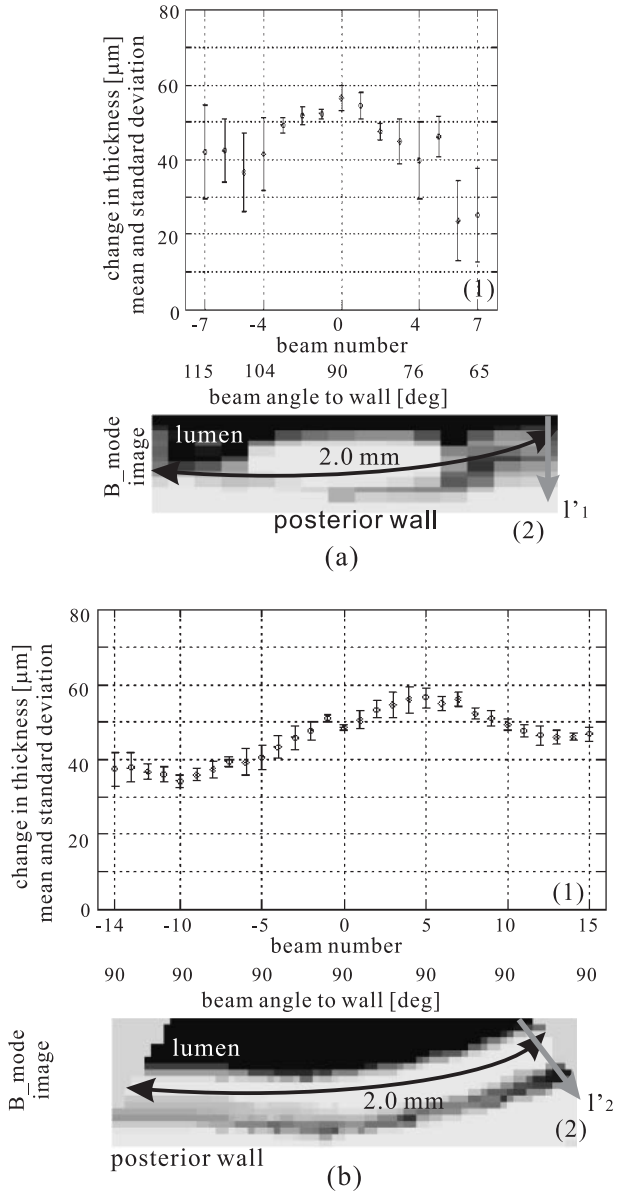

Fig. 11. (a) Measurement by the conventional linear scanning method. (b) Measurement by the proposed method. (1) Mean value and standard deviation of the maximum change in wall thickness. (2) B-mode image of the corresponding region.

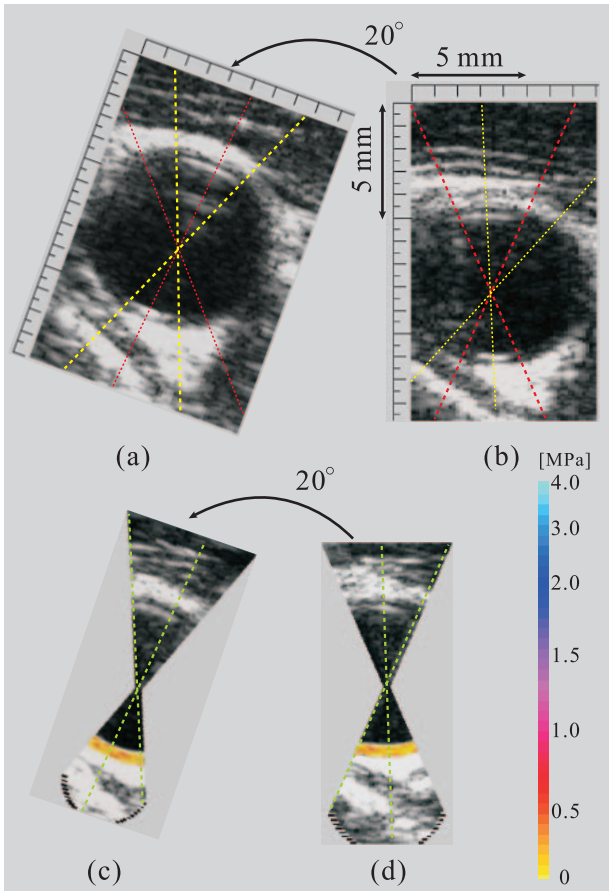

Fig. 12. (a) and (b) are B-mode images of the carotid artery in the short-axis plane obtained by the conventional linear scanning method. (c) Cross-sectional elasticity image measured from the direction shown with yellow lines in (a). (d) Cross-sectional elasticity image measured from the direction shown with red lines in (b).

tube, changes in wall thickness were accurately measured along all scan lines by the proposed method, and the measured elastic modulus agreed well with that obtained by the static experiment. In *in vivo* experiments, the change in thickness could not be accurately measured in the region where echo from the lumen-intima interface was not recognized by the conventional linear scanning method. Using the proposed method, however, the echo from the lumen-intima interface was clearly recognized and the change in thickness was measured with high reproducibility along each scan line. From the minute change in wall thickness measured at each beam position, the cross-sectional image of elasticity was obtained in the short-axis plane by the proposed method.

1) R. T. Lee, A. J. Grodzinsky, E. H. Frank, R. D. Kamm and F. J. Schoen: Circulation **83** (1991) 1764.
2) H. Kanai, M. Sato, Y. Koiwa and N. Chubachi: IEEE Trans. UFFC **43** (1996) 791.
3) H. Kanai, H. Hasegawa, M. Ichiki, F. Tezuka and Y. Koiwa: Circulation **107** (2003) 3018.
4) H. Hasegawa, H. Kanai and Y. Koiwa: Jpn. J. Appl. Phys. **41** (2002) 3563.
5) H. Hasegawa, H. Kanai, N. Hoshimiya and Y. Koiwa: Jpn. J. Med. Ultrason. **28** (2001) 3 [in Japanese].
6) C. L. de Korte, E. I. Céspedes, A. F. W. van der Steen and C. T. Lanc: Ultrasound Med. Biol. **23** (1997) 735.
7) C. L. de Korte, M. Sierevogel, F. Mastik, C. Strijder, J. A. Schaar, E. Velema, G. Pasterkamp, P. W. Serruys and A. F. W. van der Steen: Circulation **105** (2002) 1627.
8) H. Mita, H. Kanai, Y. Koiwa, M. Ichiki and F. Tezuka: Jpn. J. Appl. Phys. **40** (2001) 4753.
9) M. Watanabe, H. Hasegawa and H. Kanai: Jpn. J. Appl. Phys. **41** (2002) 3613.
10) M. Watanabe and H. Kanai: Jpn. J. Appl. Phys. **40** (2001) 3918.